CHAPTER ELEVEN

Secondary Structures of Iron Meteorites

As discussed in the previous chapter, the coarse precursor austenite crystals and the diffusion controlled Widmanstätten structure indicate high initial temperatures in the austenite region followed by extremely slow cooling. Therefore, at one time, the iron meteorites must have resided inside a parent body of some considerable size, well insulated against thermal losses and well shielded from cosmic radiation. It is now generally assumed that the parent bodies were of sizes ranging from 10-800 km in diameter. Whether the iron meteorites came from the interior mantle or from the core of one or more parent bodies is still open to dispute. It will be assumed here as a working hypothesis that the iron meteorites originated within a number of physically separated buns or more or less vertical dikes which were distributed at kilometer-depths within several parent bodies. They were probably overlain by sintered or melted, shock-metamorphosed rocks of mainly silicate composition. Whatever the assumption, the parent bodies must have been exposed to severe shocks in order to have become disintegrated so that they delivered the relatively small fragments which we now examine as meteorites.

It appears plausible that the surfaces of the parent bodies were repeatedly hit by other celestial bodies while the iron meteorites to-be were still buried at some depth. Progressive stages of shock metamorphism were thereby introduced in near-surface rocks; possibly the more deeply seated iron parent bodies were also influenced to some degree.

Finally, a particularly violent collision must have occurred and disrupted the planetoid. Most likely the relatively small "projectile" was almost entirely lost by vaporization during the impact; see page 33. Sizable fragments – perhaps some tens to thousands of meters in diameter – could, however, survive from the impacted body, preserving a range of altered structures according to their distance from the point of impact. In orbit, the fragments might suffer further collisions and even to a minor degree become periodically reheated when near the perihelia of the orbit. See page 13. Eventually, as in the case of Canyon Diablo, Morasko and other crater-producing meteorites, some meteoroids were again shocked during impact with the Earth. Usually the kinetic energy was insufficient for any violent damage to occur during terrestrial impact; the bulk of most iron meteorites display structures that were acquired at preterrestrial events.

The purpose of the present discussion is to find criteria which could serve to classify the secondary structures and thereby correctly place them in time and space. However, since the meteorites in our collections only represent a small and perhaps biased selection of the various fragments, it is often difficult to arrive at a useful classification.

It is thus quite obvious that the present subdivision is only an initial attempt and is far from exhaustive. One thing is clear, however: the iron meteorites present, even within the same chemical group, a surprisingly large variation in secondary structures and the underlying causes and events must have been rather complex; i.e., cycles of cooling and reheating, shocking and plastic deformation must have occurred on different intensity levels at various times. More criteria than used here, e.g., noble gas data and fission tracks, will eventually have to be applied to elucidate the events and permit more accurate conclusions.

The surprisingly large number of iron meteorites which have been exposed to artificial deformation and reheating are not discussed here. Criteria to distinguish these effects from genuine cosmic effects have been established and discussed on page 40 and in numerous places under the individual descriptions.

The secondary structures observed in iron meteorites may conveniently be divided into four main categories that somewhat overlap: (i) those caused by shock-induced plastic deformation, (ii) those caused by shock-induced solid state transformation, (iii) those caused by shock melting and (iv) those caused by thermal annealing, either due to shock relaxation or to orbital reheating in the perihelia. The secondary structures are, geologically speaking, metamorphic structures.

In terrestrial rocks the secondary metamorphic structures caused by meteorite impacts have been thoroughly studied since about 1960. See, e.g., French & Short (1968) and Stöffler (1971b). The metamorphism in chondrites has been well studied and even used as a basis for classification. See page 62. Recently, the lunar rocks have also been examined for an abundance of shock effects. See, e.g., Mason & Melson (1970), Short (1970) and Anderson (1973). The presence of quartz and framework silicates, e.g., feldspar, have greatly assisted in the interpretation of the secondary structures of rocks and breccias from impact sites. Iron meteorites do not contain a sufficient amount of these shock indicators to be of importance in the study. Instead, interest must center upon kamacite, diamond,

cohenite, schreibersite and troilite; and important contributions have come from, e.g., Brentnall & Axon (1962), El Goresy (1965), Heymann et al. (1966), Lipschutz (1968), Axon (1969), Zukas (1969) and Jain & Lipschutz (1970). For a general discussion of the effects of explosive shock on crystalline solids, the reader is referred to, e.g., Dieter (1962), Leslie et al. (1962), Leslie et al. (1965), Doran & Linde (1966) and De Carli (1968).

(i) Shock-Induced Plastic Deformation

At relatively low rates of deformation the metallic matrix is cold-worked and the included minerals distorted and brecciated. Deformation rates and heating of the required low degree may have occurred in a hemispherical zone farthest away from the impact center on the parent body; see Figure 200. Relatively low deformation rates also apply to the breakup of an average meteorite in the Earth's atmosphere, and to bulk deformation processes of a geological character on the parent body.

1. Kamacite. It will be assumed that the kamacite at the end of the primary cooling period was thoroughly annealed and exhibited minimum of hardness – i.e., a 7% Ni kamacite showed a microhardness of 155±5 Vickers. Many meteorites, however, now display significantly higher hardness values, up to 325±25, because they have been exposed to subsequent cold working. In Joe Wright Mountain, e.g., the high hardness appears to be the result of preatmospheric shock-deformation. But in Cape York and Campo de Cielo the hardening is almost certainly the result of the combined effect of planetary breakup and the plastic deformation caused by atmospheric disruption. The deformation bands in the kamacite near necked portions of the latter are very distinctive for atmospheric breakup. In fact, if one should observe necked near-surface portions with deformation bands on a new find, it is recommended that a field search be instigated for the missing fragments.

Shock pressures above 10 k bar but below 130 k bar will cause simple twinning, with the twin density increasing as the shock pressure is increased. The number of dislocations, which simultaneously increases, must be assumed to be the direct reason for the observed significant hardness increase in shocked samples. In a preliminary electron-microscopic study of shock-deformed material from Cape York, kamacite with a microhardness of 250 Vickers was found to have a dislocation density of 10^9 l/cm^2. The dislocations formed irregular tangles and networks, and a major portion could be shown to be screw dislocations. See Figures 101 and 102 and Jago (1974).

Under the microscope the mechanical twins appear as Neumann bands parallel to $(112)_\alpha$, but usually not all of the possible twinning planes have been in operation. The appearance of the kamacite depends upon the orientation of the observed crystal relative to the plane of sectioning. The microhardness of the kamacite also depends on the orientation and moreover on the orientation of the indenting pyramid relative to the cubic crystal. The lowest hardness is always recorded when the impression takes on a pincushion shape, while the highest is associated with a barrel shape. A variation of ±10% may alone be ascribed to this orientation effect. For a thorough discussion of this aspect the reader is referred to Bückle (1959).

Most Neumann bands in meteorites have extraterrestrial causes. They are often decorated by small particles caused by subsequent cosmic reheating. A few minor bands, usually located near internal cracks, have apparently been produced during the atmospheric disruption.

In many cases microcracks are present in the kamacite of both hexahedrites and octahedrites. The cracks, which as a rule first become visible when well polished samples are examined, usually follow $(100)_\alpha$ cubic cleavage planes of the kamacite. They are referred to in the text as "cubic microcracks."

2. Taenite. At the end of the primary cooling period the taenite was zoned and annealed to a hardness of about 155±5 (~ 30% Ni). If subsequently exposed to low deformation rates, it became kneaded and distorted to a hardness of 300-400. The hardness is always found to be appreciably

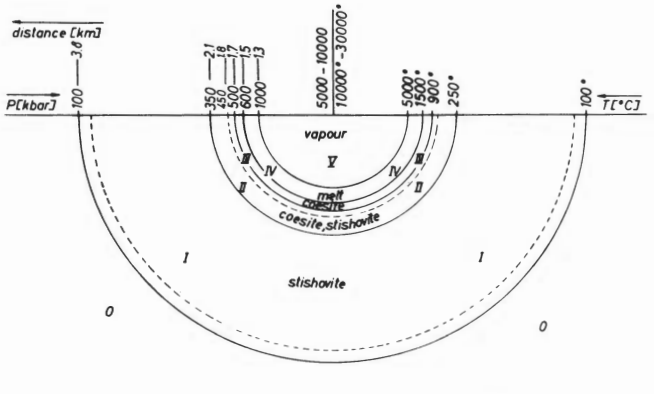

Figure 200. Schematic representation of the different zones of shock metamorphism on a planetary surface. Peak pressures are in kilobars, and temperatures are post-shock temperatures. Formation conditions for coesite and stishovite from quartz are indicated. (From Stöffler 1971a.)

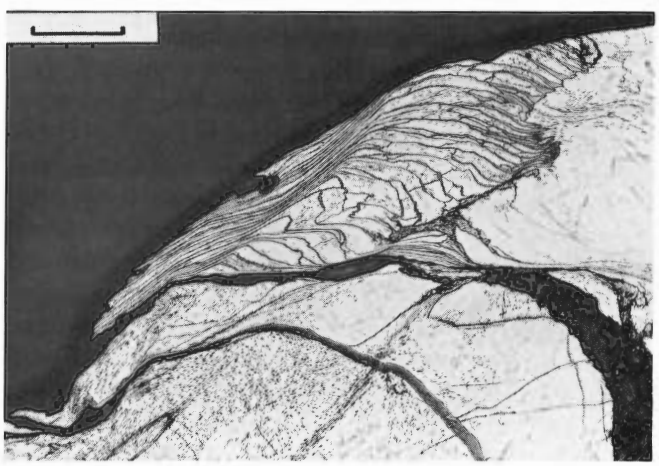

Figure 201. Cape York (Woman, New York). Severe necking and shear-deformation in near-surface areas of many meteorites suggest a violent disruption in the atmosphere. The kamacite hardness increases here to about 250 Vickers. Etched. Scale bar 300 μ.

higher than in the coexisting kamacite; i.e., the taenite has a larger coefficient of work hardening than kamacite. This is perhaps not surprising for a face centered cubic phase compared to a body centered cubic phase.

At high shock pressures the taenite responds by developing extreme hardness. It appears that a number of densely spaced slipplanes parallel to $(111)_\gamma$ are activated. These may often be detected by application of an oil immersion objective to a thoroughly polished and etched section, e.g., Veliko-Nikolaevskij Priisk. The slipped regions abut along a number of steps against the distorted kamacite that has usually transformed to the hatched ϵ-variety. Peak hardnesses of 475±25 have been observed in shock-deformed taenite of many irons, e.g., Cranbourne, Osseo and Canyon Diablo. The hardest taenite is usually found in irons of group I where the deformation hardness is probably enhanced by carbon in solid solution in the taenite. Odessa samples, that were shocked by De Carlie to peak pressures of 1000 k bar and examined for their hardness distribution during the present work, showed maximum taenite hardness of 560±30. See Figure 205.

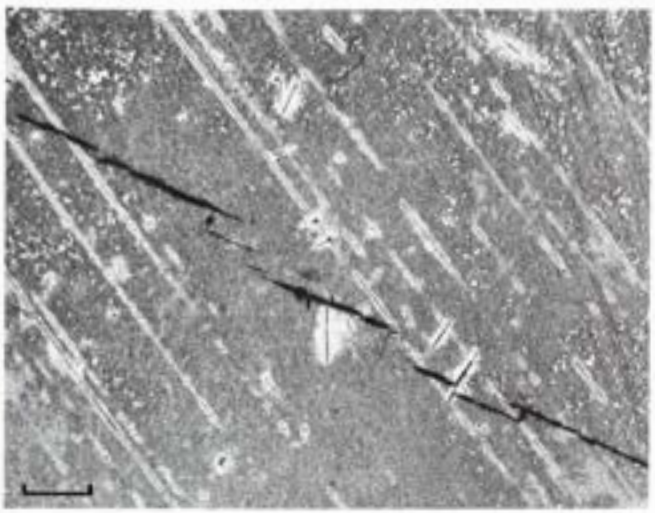

Figure 202. Sierra Gorda (U.S.N.M. no. 1307). A typical hexahedrite. The spotted appearance is mainly due to variation in numbers and sizes of phosphide precipitates. Decorated Neumann bands. Microfissures along cubic cleavage planes. Etched. Scale bar 1 mm.

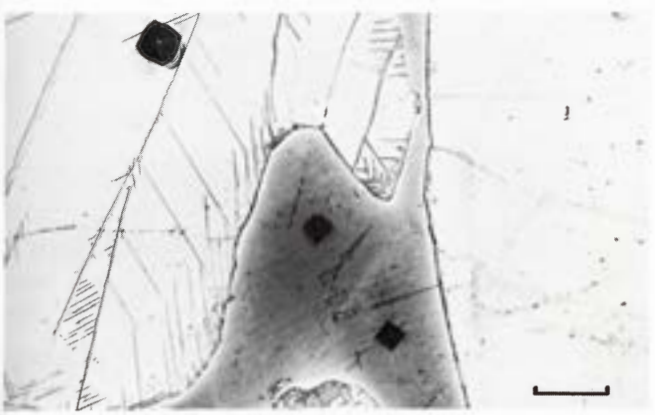

Figure 203. Odessa, artificially shocked to peak pressures of 800 k bar. Microhardness indentations in kamacite and taenite. Etched. Scale bar 50 μ.

3. Troilite. At the end of the primary cooling period the troilite was monocrystalline and exhibited sharp boundaries against the surrounding metal. This type is designated "1" in Appendix 1. Mild plastic deformation caused mosaicism in the troilite – i.e., the previously homogeneous crystal became divided into cells, 10-500 μ in size, with unusually strong and irregular undulatory optical extinction. This type is designated "3" in Appendix 1. Brecciation effects and shear-deformation may also be noted, especially where troilite is in contact with daubreelite, chromite, cohenite or schreibersite.

In more strongly shocked specimens the troilite deformed by multiple twinning. Since this form usually occurs together with kamacite of the shock-hatched type, it appears that it requires average shock pressures of about 150 k bar for its formation. The twinned troilite is designated "2" in Appendix 1, and typical examples are found in Savannah, Augusta County, Rateldraai and Tawallah

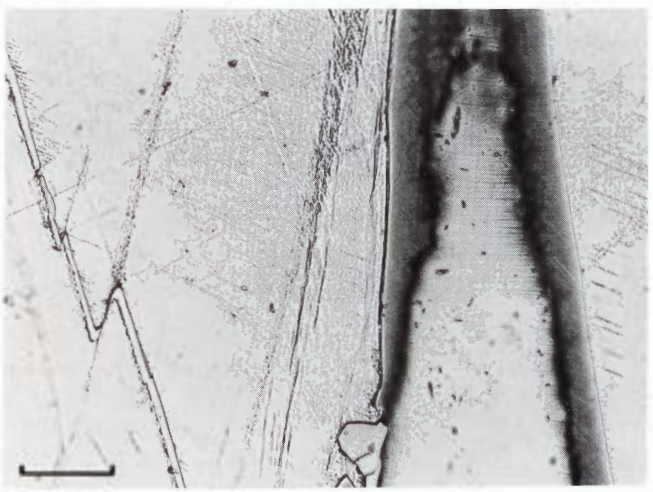

Figure 204. Odessa, artificially shocked to peak pressures of 800 k bar. Severe shear-deformation has bent a narrow taenite lamella (left), while numerous $(111)_\gamma$ slipplanes have been introduced in the thicker one. Etched. Scale bar 40 μ.

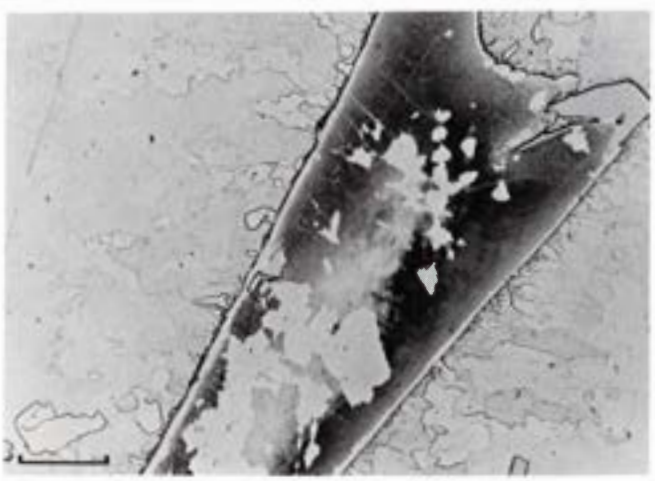

Figure 205. Odessa, artificially shocked to peak pressures of 1000 k bar. Slipplanes are visible in the cloudy taenite. Because of the shock relaxation reheating the taenite shows white patches in a mosaic pattern. Compare Figure 53. Etched. Scale bar 40 μ.

Valley, all of which are believed to have been exposed to preterrestrial shock effects.

4. Bulk deformation. As mentioned above under 1, broad deformation bands and shear zones are seen in numerous meteorites. When present in large, shower- or crater-producing meteorites, the damage may usually be attributed to the disruption and impact event itself. This is true of most of the deformation seen in Canyon Diablo, Campo del Cielo, Gibeon, Glorieta Mountain, Cape York, Henbury and Imilac.

Similar deformation structures are, however, also present in small irons which were not exposed to violent forces during terrestrial impact. The incredible shear deformations of Chinga, New Baltimore and Muzzaffarpur must thus represent some preterrestrial event, possibly when confined to the parent body and situated in the exterior zone of alteration associated with impact.

Less severe deformation structures are present in, e.g., Puquios, Charcas, Tombigbee, Tamarugal, Kodaikanal, Nelson County and Sacramento Mountains. The effects are no doubt preterrestrial, as proved both by the intensity of the damage and by the occasional recrystallization of kamacite along shear zones and precipitation of phosphides on the defects during subsequent annealing.

(ii) Shock-Induced Solid State Transformations

At high shock pressures several minerals may transform to more dense modifications. Quartz forms stishovite and coesite (Chao et al. 1960; 1962) that can remain as metastable phases in the shocked material and may subsequently be used as shock indicators. During the shock feldspar may become completely transformed to a high pressure phase; this reverses, however, on pressure release to an amorphous, low density glass which is called maskelynite (Tschermak 1872c; Milton & De Carli 1963) or diaplectic feldspar glass (von Engelhardt & Stöffler 1968). In iron meteorites, the shock-transformation of graphite to diamond corresponds to the coesite case while the formation of hatched kamacite slightly corresponds to the feldspar reversion. It is possible that an examination of iron meteorites with silicate inclusions might reveal shocked structures in the feldspars.

1. Kamacite. If a shock pressure of about 130 k bar is reached or exceeded, the kamacite transforms diffusionless to hexagonal close-packed ϵ-iron of high density (Smith 1958; Maringer & Manning 1962; Takahashi & Bassett 1964). In experiments conducted at static pressures, the density of the α-phase increases gradually from 7.86 at 1 atmosphere to 8.46 g/cm^3 at 130 k bar, then jumps abruptly to 8.81 g/cm^3 at the phase transition. Upon pressure release, the ϵ-phase reverses to α. The resulting distorted structure appears hatched and somewhat resembles martensite on a polished and etched section. It has been termed ϵ in most places in the descriptive part of this handbook, although, sensu strictu, it is *now* a distorted α-phase. The microhardness is anomalously high, 300-350 Vickers (100 g

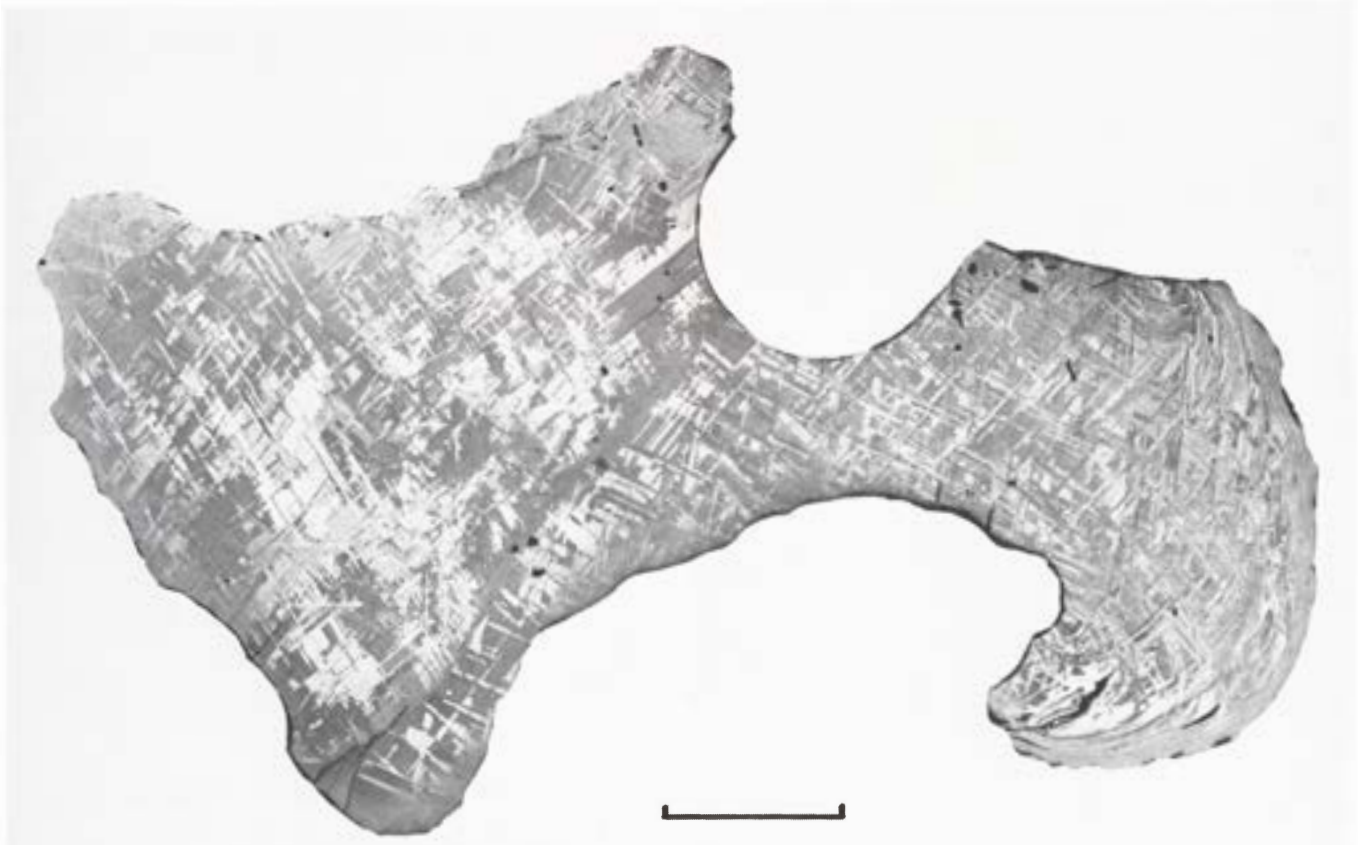

Figure 206. Gibeon (U.S.N.M.; Bosch Collection no. M-578). A violent torsional fracture (right) separated this Gibeon mass from another during atmospheric breakup. Etched. Scale bar 50 mm. S.I. Neg. M-1438.

Valley, all of which are believed to have been exposed to preterrestrial shock effects.

4. Bulk deformation. As mentioned above under 1, broad deformation bands and shear zones are seen in numerous meteorites. When present in large, shower- or crater-producing meteorites, the damage may usually be attributed to the disruption and impact event itself. This is true of most of the deformation seen in Canyon Diablo, Campo del Cielo, Gibeon, Glorieta Mountain, Cape York, Henbury and Imilac.

Similar deformation structures are, however, also present in small irons which were not exposed to violent forces during terrestrial impact. The incredible shear deformations of Chinga, New Baltimore and Muzzaffarpur must thus represent some preterrestrial event, possibly when confined to the parent body and situated in the exterior zone of alteration associated with impact.

Less severe deformation structures are present in, e.g., Puquios, Charcas, Tombigbee, Tamarugal, Kodaikanal, Nelson County and Sacramento Mountains. The effects are no doubt preterrestrial, as proved both by the intensity of the damage and by the occasional recrystallization of kamacite along shear zones and precipitation of phosphides on the defects during subsequent annealing.

(ii) Shock-Induced Solid State Transformations

At high shock pressures several minerals may transform to more dense modifications. Quartz forms stishovite and coesite (Chao et al. 1960; 1962) that can remain as metastable phases in the shocked material and may subsequently be used as shock indicators. During the shock feldspar may become completely transformed to a high pressure phase; this reverses, however, on pressure release to an amorphous, low density glass which is called maskelynite (Tschermak 1872c; Milton & De Carli 1963) or diaplectic feldspar glass (von Engelhardt & Stöffler 1968). In iron meteorites, the shock-transformation of graphite to diamond corresponds to the coesite case while the formation of hatched kamacite slightly corresponds to the feldspar reversion. It is possible that an examination of iron meteorites with silicate inclusions might reveal shocked structures in the feldspars.

1. Kamacite. If a shock pressure of about 130 k bar is reached or exceeded, the kamacite transforms diffusionless to hexagonal close-packed ϵ-iron of high density (Smith 1958; Maringer & Manning 1962; Takahashi & Bassett 1964). In experiments conducted at static pressures, the density of the α-phase increases gradually from 7.86 at 1 atmosphere to 8.46 g/cm^3 at 130 k bar, then jumps abruptly to 8.81 g/cm^3 at the phase transition. Upon pressure release, the ϵ-phase reverses to α. The resulting distorted structure appears hatched and somewhat resembles martensite on a polished and etched section. It has been termed ϵ in most places in the descriptive part of this handbook, although, sensu strictu, it is *now* a distorted α-phase. The microhardness is anomalously high, 300-350 Vickers (100 g

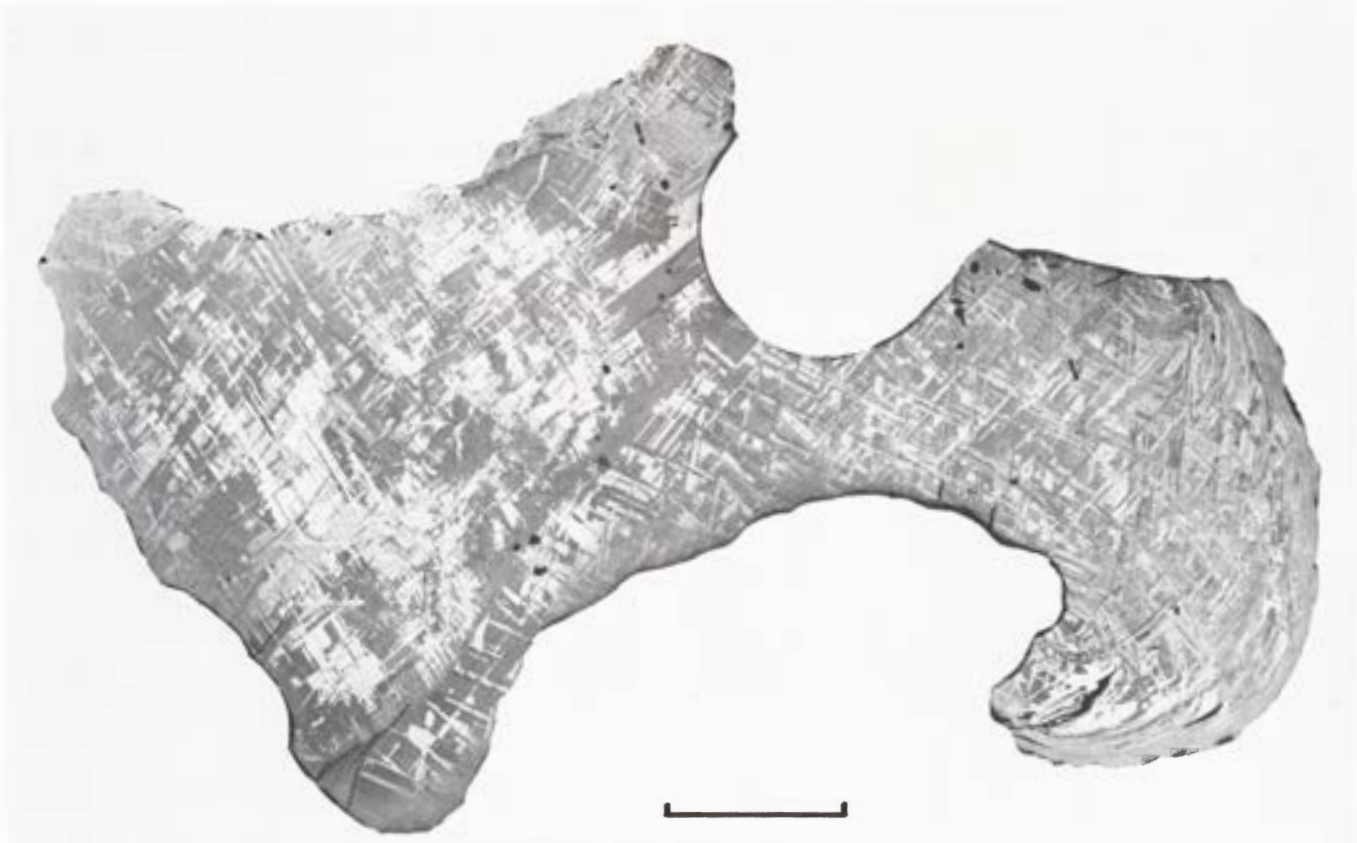

Figure 206. Gibeon (U.S.N.M.; Bosch Collection no. M-578). A violent torsional fracture (right) separated this Gibeon mass from another during atmospheric breakup. Etched. Scale bar 50 mm. S.I. Neg. M-1438.

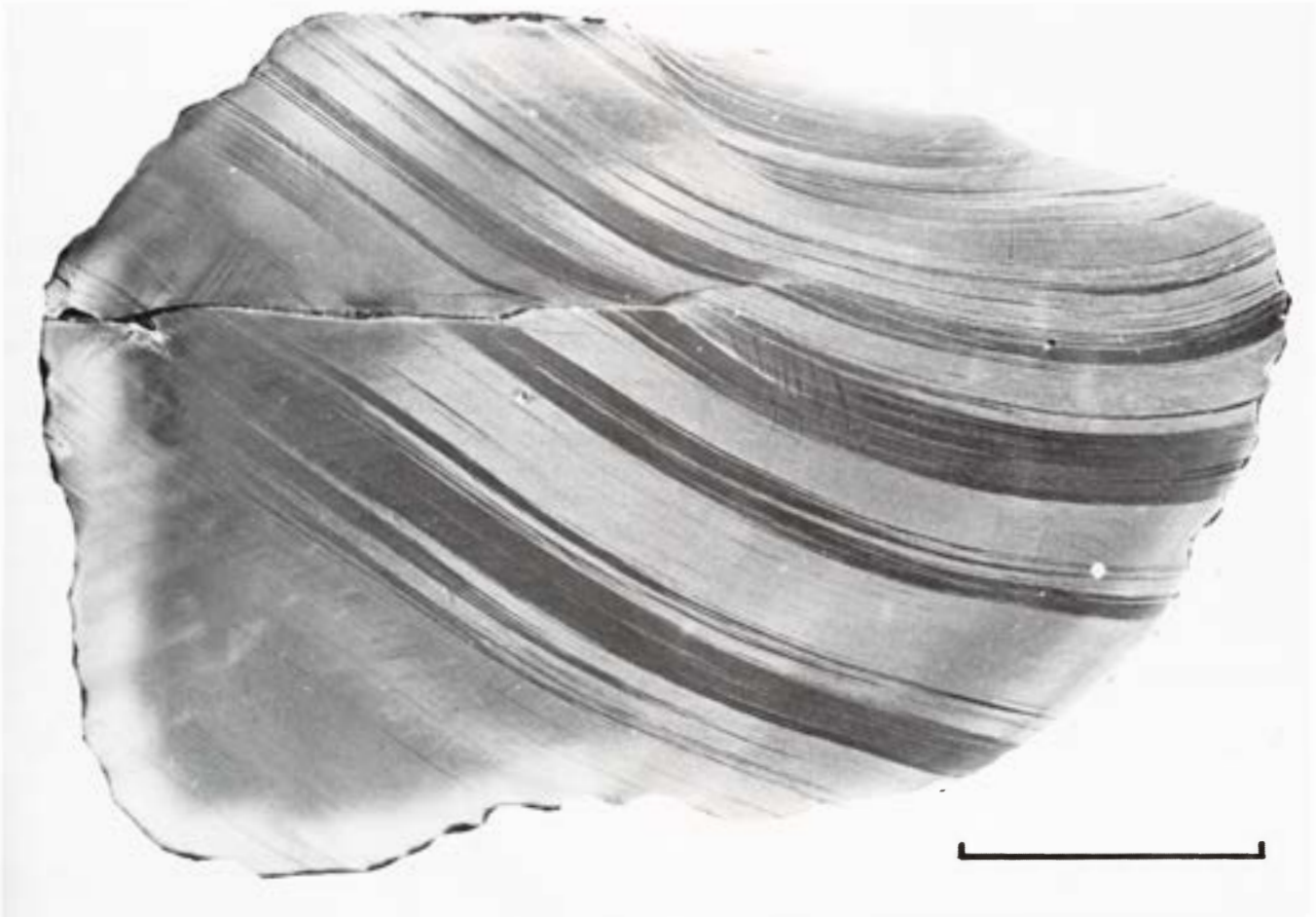

Figure 207. Chinga (U.S.N.M. no. 3451). Severe preterrestrial shock-deformation shear displaced part of the mass and bent all of it, as indicated by the distorted Schlieren bands. Etched. Scale bar 20 mm. S.I. neg. M-1342.

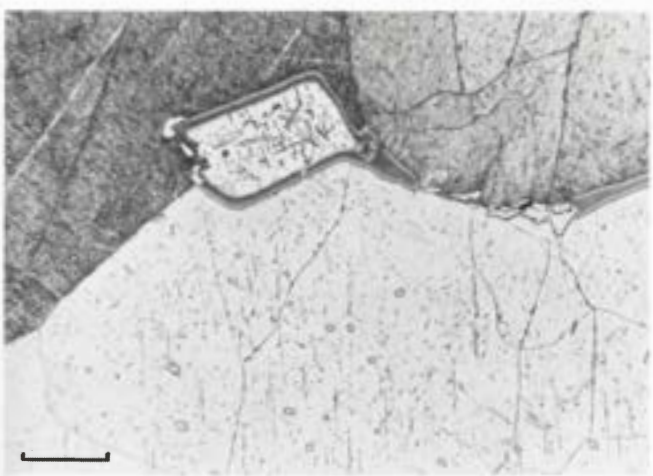

Figure 208. Odessa, artificially shocked to peak pressures of 200 k bar. Three differently oriented kamacite lamellae exhibit different shades of shock-hatched ϵ-structures, but all display the same microhardness. Etched. Scale bar 200 μ.

load). As is the case for the Neumann bands, the hatched structure is differently developed on differently oriented crystal faces, giving rise to matte structures of various appearance. Zukas et al. (1963) have, for instance, presented photomicrographs of the appearance of the transformation structure on differently oriented sections. Lipschutz & Jaeger (1966) have examined the shock damage by X-ray diffraction spectroscopy.

Examination of a number of Odessa samples shocked to peak pressures of 200, 400, 600, 800 and 1000 k bar by De Carli and loaned to me, yielded the hardness band shown in Figure 112. It is apparent that the hardness increases abruptly when the transformation pressure is reached. Although the data are very limited as yet and steep pressure gradients are noted in the studied sections, the trend is nevertheless clear. The simultaneous measurement of α and γ and optical examination of included troilite should provide a powerful means of elucidating the peak shock pressures. It is remarkable how common the shock-hardened, hatched ϵ-structures are in group IIIA-IIIB, where about 80% of all meteorites exhibit them in one or another variety. On the other hand, ϵ is absent in group IIA and I – except in shower- and crater-forming meteorites – and very rare in the anomalous meteorites. The ϵ also seems to be absent in the kamacite of stone meteorites (Heymann 1967). The occurrence of the shock-hardened phase is noted in column 9 of Appendix 1.

2. Taenite. The response of taenite to high shock pressures is not well known. However, as is clear from

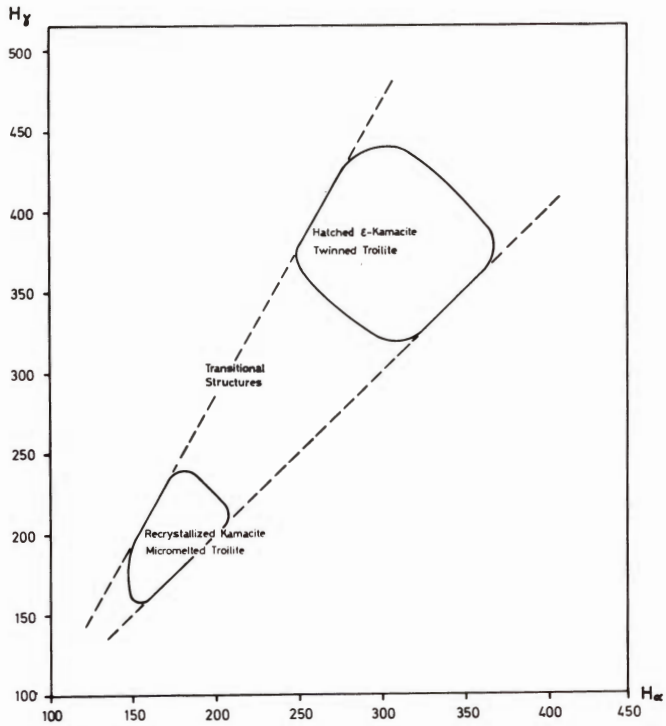

Figure 209. Microhardness of taenite plotted versus microhardness of kamacite for a large number of meteorites. The appearance of kamacite and troilite in the measured samples is also indicated. Compare Figure 111.

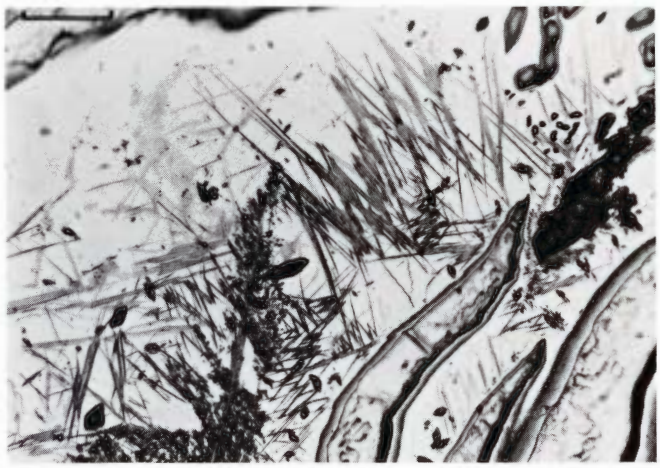

Figure 210. Odesa, artificially shocked to peak pressures of 600 k bar. A previously homogeneous taenite field with about 25-30% Ni now exhibits acicular martensite transformation products, due to shock. Etched. Scale bar 40 μ.

Figure 112, its hardness increases smoothly with shock pressure, and there are no indications of shock-transformations. Odessa samples, exposed in the laboratory to 600 k bar and above, sometimes exhibit well developed acicular martensite inside former homogeneous taenite areas, Figure 210. It appears that this martensite formed during the decompression stage after the shock wave had passed and only developed inside taenite with 25-30% Ni and some carbon in solid solution.

3. Graphite. Although graphite is present in numerous iron meteorites (See page 109 and Appendix 1.), there is only one well documented example that it has transformed to diamond, namely, in Canyon Diablo. It serves here to show that certain fragments of the Earth-impacting meteorite were intensively shocked and shock-reheated whereby graphite associated with troilite converted to diamond and lonsdaleite. See page 385.

(iii) Shock-Induced Melting

High shock pressures may, by reflection and attenuation of the shock wave at grain- and phase-boundaries and external surfaces, lead to local "hot spots." Selective melting of silicates and quartz may thereby occur and produce glass.

In iron meteorites troilite is a sensitive mineral, apparently because it is more compressible than the surrounding metal and acts as a shock absorber. It heats appreciably and is usually of small volume and inferior heat conductance, so it may completely melt in situ. The

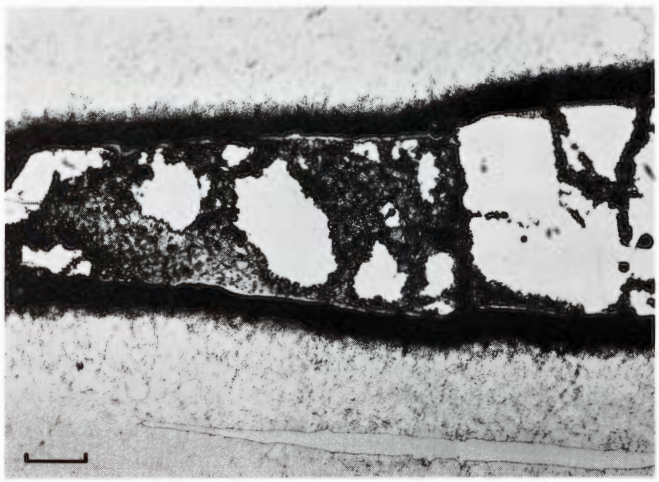

Figure 211. Canyon Diablo (Copenhagen no. 121264). A small shocked and annealed sample from the crater field. The cohenite crystal is partly melted, and carbon has diffused 50 μ outwards into adjacent metal. Compare Figures 212, 213, 475 and 476. Etched. Scale bar 100 μ.

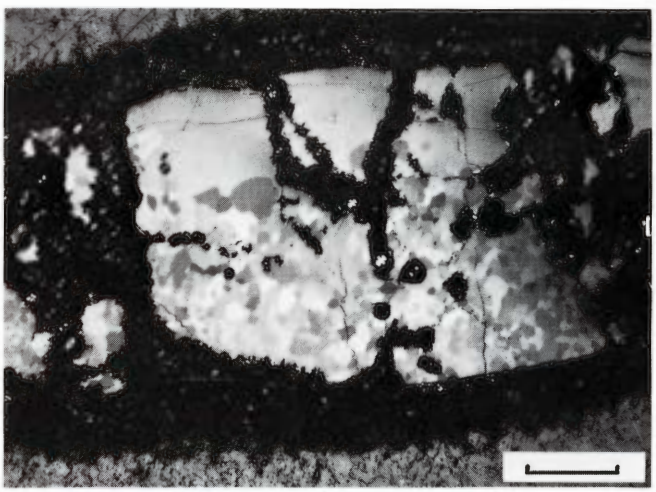

Figure 212. Detail of Figure 211 under crossed polars. The surviving cohenite is recrystallized. The numerous white dots in the black matrix are graphite spherulites in a ledeburitic-steaditic melt. See Figure 213. Scale bar 100 μ.

melting point of pure troilite is about 1190° C (Hansen & Anderko 1958). When associated with α-iron, cohenite and schreibersite, the melted troilite may react and form characteristic binary and ternary eutectics with up to 200° C lower melting points. Cracks which form simultaneously in the adjacent metal and minerals may become filled with rapidly injected troilite melts. It even appears that the rapidly formed and unequilibrated Fe-S-P liquids may solidify as disordered glasslike droplets, dispersed in metallic eutectics.

The associated minerals (cohenite, graphite, schreibersite, daubreelite, chromite and silicates) are either fragmented and dispersed through the liquid, or even partially melted (schreibersite, daubreelite, cohenite), thereby forming eutectic fine-grained structures of a ledeburitic appearance (Figure 212). Sometimes cohenite is decomposed to α-iron and graphite which is dispersed as minute spherulites (~ 10 μ) through the mixed melts. See, e.g., Canyon Diablo, stage VII.

The shock-melted troilite is designated "5" in Appendix 1. It is evidently quite common. By macroscopic examination of polished sections, it is observed as matte, somewhat blurred spots with internal flow lines and diffuse serrated edges against the surrounding metal. The shock-melted troilite is almost always due to preterrestrial shock events, as evidenced by the associated structures of the metal and other minerals.

Meteorites exhibiting *bulk melting* as a result of shock events on the parent body are very rarely observed. First, the volume of such material relative to less damaged material must have been small from the beginning. Second, such material was perhaps immediately reduced to sizes which would have little chance to survive atmospheric entry on Earth. Nedagolla is, however, a unique meteorite which may represent remelted and rapidly solidified material.

A few meteorites exhibit altered structures which may be attributed to shock-reheating close to the melting point

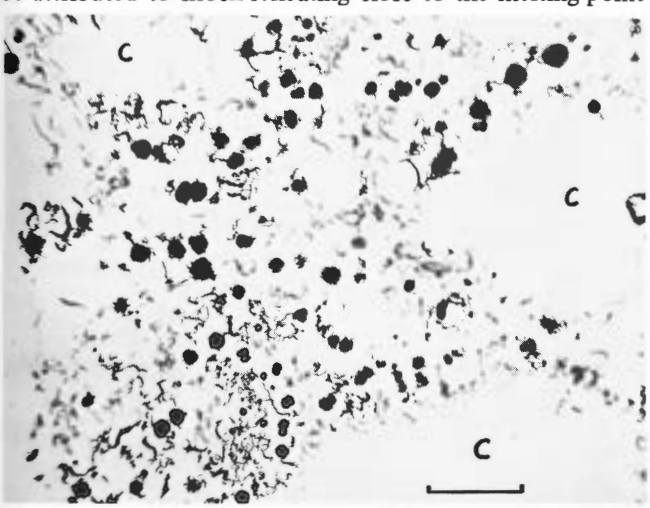

Figure 213. Detail of Figures 211 and 212, polished only. The melts between untransformed cohenite (C) are extremely fine-grained and alternate rapidly between "gray cast iron with flaky graphite" and "nodular cast iron with spherulitic graphite." Graphite is black in photo. Scale bar 40 μ.

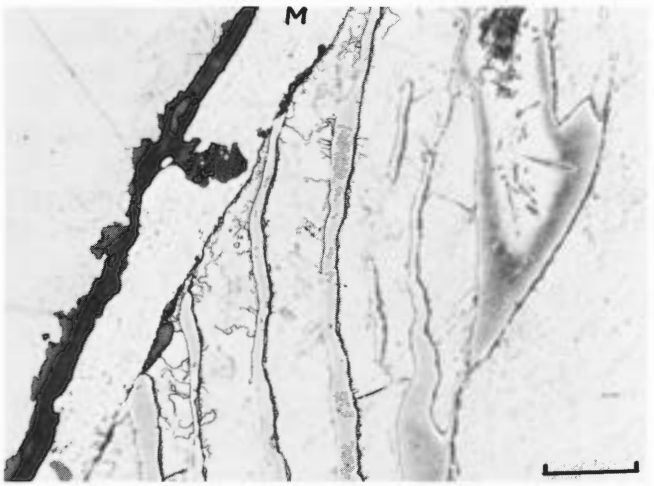

Figure 214. Odessa, artificially shocked to peak pressures of 800 k bar. The kamacite phase is transformed to α_2 and shock-melted mixtures (M) of troilite, phosphide, metal and limonite penetrate along grain boundaries. Etched. Scale bar 40 μ.

of the metal and exceeding the melting point of several of the included minerals. Candidates to this category are, e.g., Smithland, Juromenha, Ternera, Santiago Papasquiaro, Rafrüti and Mejillones. Examples may thus be found within most of the chemically resolved groups.

(iv) Thermally Altered Structures

Any of the above discussed categories i-iii may, due to circumstances, later have been exposed to annealing. The *artificial* annealing was discussed on page 40 and will not be considered further. At least four other modes of annealing can be visualized, either singly or in succession. One occurred inside the parent body, another in orbit, the third during atmospheric penetration, and the fourth during crater formation *on Earth*.

We will accept the principle of progressive shock metamorphism, which in the case of an impact on the surface of the parent body postulates gradually decreasing shock compression of approximately hemispherical geometry radiating outward from the point of impact. The rock volume and the buried parent iron meteorite bodies will thus exhibit shock metamorphism which decreases in intensity with distance from the impact center. Several impact events may have occurred before a final violent one disintegrated most of the body and the meteoroids were released. Since the material while buried, a priori, had its maximum size and its best thermal insulation, any shock-reheating would be slowly dissipated and operate through large volumes. The effects are comparable to long term annealing of deformed material at relatively low temperatures; i.e., close to or somewhat above the recrystallization temperatures. The resulting structures are recovered or polygonized or recrystallized according to the precise size, history and composition of the meteorite parent body.

During orbital life periodical reheating occurred in the perihelial part of the orbits. This effect would presumably recur a number of times with approximately equal intensity. Recovery, and perhaps recrystallization, might occur

in favorable cases, and hydrogen and helium-3 from cosmic radiation could be driven out by the reheating. For the time being it is difficult to distinguish between reheating inside the parent body and reheating in orbit. Additional noble gas data will probably help to solve the problem.

The atmospheric reheating strips the exterior off the meteorite and leaves a nucleus with a 5-20 mm thick reheated exterior crust (page 53). The bulk of the average

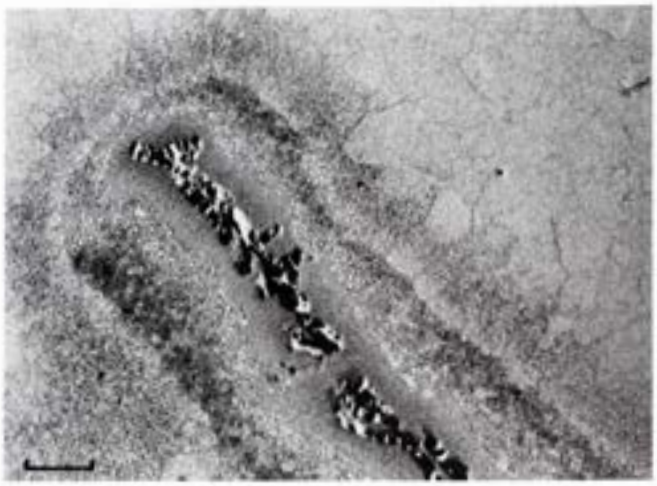

Figure 215. Mejillones (U.S.N.M. no. 734). In this meteorite there is a pronounced zoning around primary schreibersite crystals. The zones are apparently caused by secondary steep temperature – and pressure – gradients whereby nickel and phosphorus diffused outwards from the damaged schreibersite. Etched. Scale bar 1 mm.

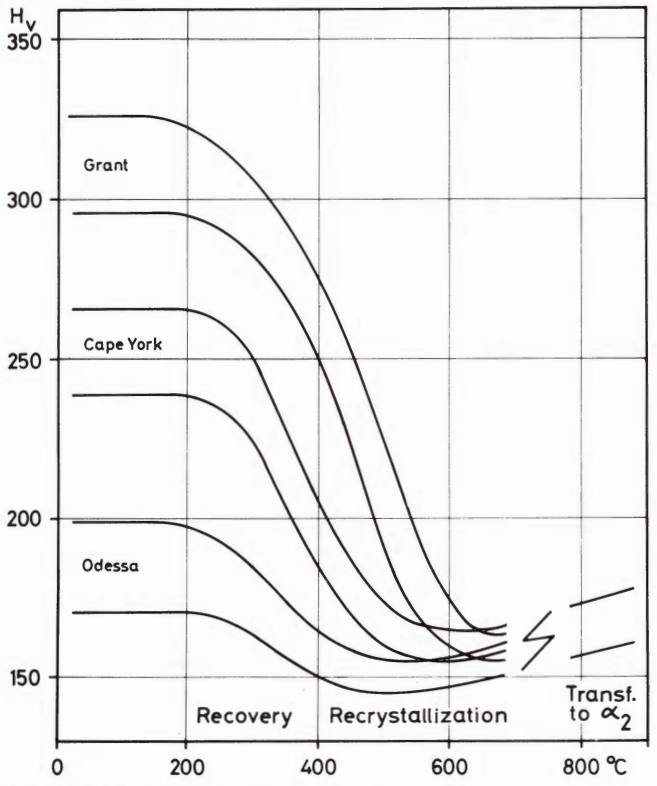

Figure 216. Preliminary results of an experimental annealing of three different iron meteorites. Microhardness (100 g Vickers) of kamacite lamellae after half an hour at temperatures indicated. Grant originally had a shock-hatched ϵ-structure, Cape York a cold-worked twinned structure and Odessa a slightly worked twinned structure.

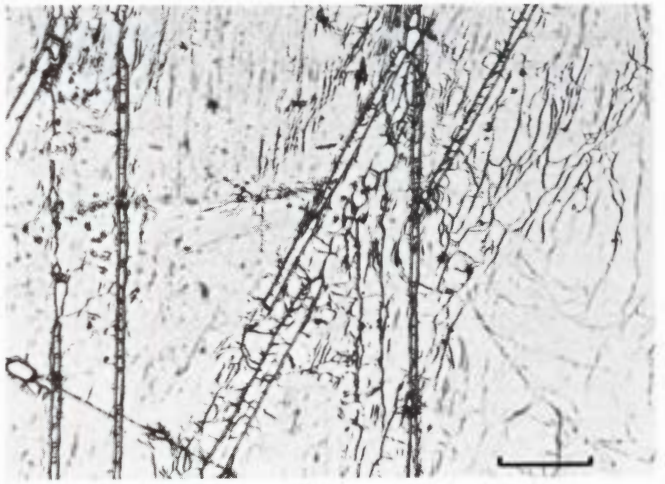

Figure 217. Willow Creek (U.S.N.M. no. 900). The kamacite is annealed to polygonization, but a portion of the Neumann bands remains. In other parts of the same meteorite 100-200 μ recrystallized kamacite grains occur. Etched. Scale bar 40 μ.

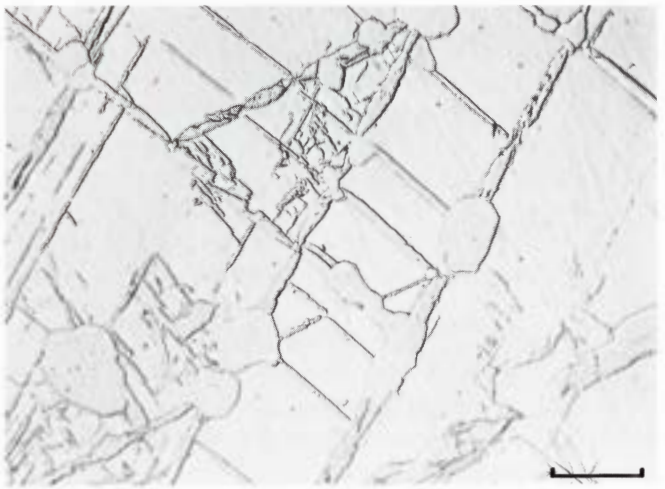

Figure 218. Avoca (Brit. Mus. no. 1968, 277). Incipient recrystallization at Neumann band intersections. The matrix is particularly strained at twin intersections, and these provide the first nuclei for recrystallization. Etched. Oblique illumination. Scale bar 20 μ.

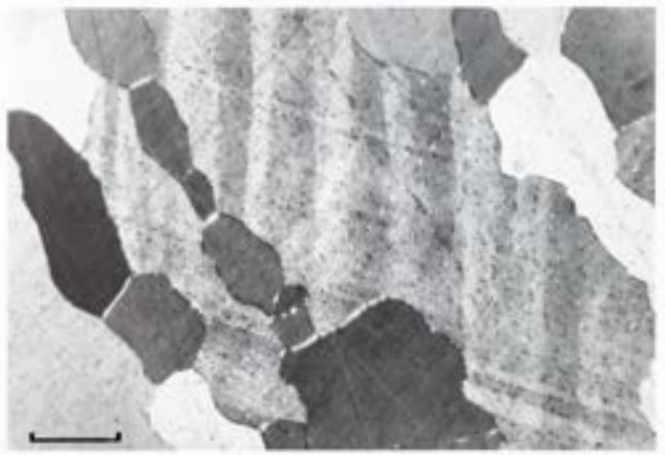

Figure 219. Joel's Iron (Brit. Mus. no. 35782). This meteorite is almost wholly recrystallized. It is typical that the new grains are elongated parallel to some of the previous Neumann band directions. Etched. Crossed polars. Scale bar 100 μ.

iron meteorite is, however, not affected by the atmospheric flight.

The crater-producing meteorites provide material of several kinds. Near-surface material which broke off high in the atmosphere and had independent flights still exhibit the unaltered cosmic structure. Material, which was part of the impacting body itself, underwent a whole range of shock metamorphism. The best studied case is that of Canyon Diablo to which the reader is referred. It is characteristic that the resulting structures are due to high shock pressures and temperatures and subsequent rapid cooling, i.e., cooling within minutes or hours to room temperature.

Although as yet difficult to prove, it is felt that the majority of the annealing effects discussed below were produced when the meteorites were still residing inside their parent bodies. A minor portion occurred in orbit, and very few occurred during cratering impact. See Table 18.

1. Kamacite. Reheating above 750° C will transform kamacite, whether deformed or undeformed, to taenite which upon cooling reverses to the distorted α_2 structure. The α_2 as a major part of the kamacite in iron meteorites is only present in the heat-affected rim zone (page 51) and in certain shower- or crater-producing meteorites, such as Gibeon, Henbury, Morasko and Canyon Diablo. The hardness of the α_2 phase is usually 30-50 units higher than the corresponding annealed kamacite. In Figure 112 the dropping tail of the kamacite curve at 800-1000 k bar is due to the presence of increasing amounts of α_2. The intermediate portion, at 400-600 k bar, is probably due to shock annealing of ϵ and to incipient recrystallization.

Deformed kamacite will upon reheating below 750° C recover or polygonize or recrystallize. These changes are conveniently followed by optical and electron microscopy, by X-ray diffraction and by hardness testing.

Laboratory experiments indicate that the microhardness of deformed kamacite is relatively easily restored to annealed values of about 155, apparently with very little alteration of the optical appearance. For example, 20 minutes at 500° C was sufficient to anneal the kamacite of Cape York, but only negligible recrystallization occurred, the bulk of the Neumann bands remaining unaltered after the annealing. Attempts to fully recrystallize the material were unsuccessful; five hours treatment at 700° C thus only recrystallized 10% of the sections. Figure 216 shows some preliminary results.

The recrystallized grains in the experimental material were mainly found at Neumann band intersections and in the plastically deformed kamacite along sheared schreibersite inclusions. Minor and slower recrystallization proceeded outwards from imperfections along the Neumann bands and the grain boundaries. From these experiments and from numerous other observations on meteorites, it appears that purely twinned material will only with difficulty recrystallize upon reheating. The twins will be more likely to disappear by reversion unless they have already become pinned by precipitates. Proper recrystallization will usually

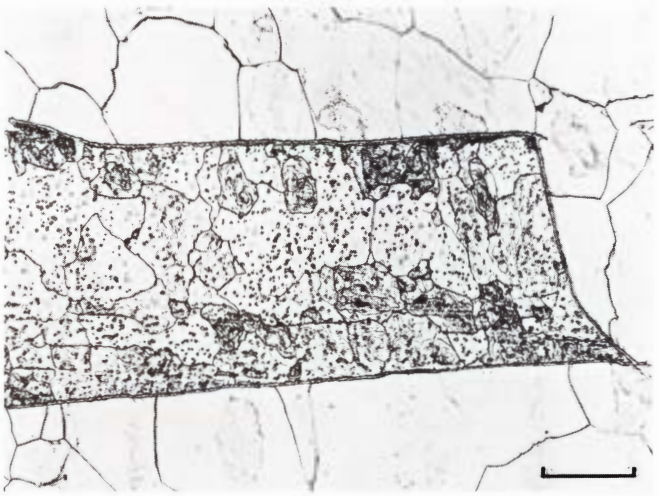

Figure 220. Social Circle (U.S.N.M. no. 1675). Fully recrystallized meteorite. Successive growth lines are present within many of the new grains, suggesting several cycles of heating and cooling. The new grains are smallest within former plessite fields because taenite particles have restricted growth somewhat. Etched. Scale bar 100 μ.

Figure 221. Tombigbee (U.S.N.M. no. 252). Recrystallized grains with new Neumann bands, probably dating from the atmospheric breakup. Etched. Scale bar 100 μ. (From Perry 1950: volume 1.)

be restricted to regions which, in addition to mechanical twinning, also exhibit significant elements of plastic deformation.

Incipient recrystallization and competition between polygonization and recrystallization is present in, e.g., the meteorites Forsyth County, Hex River, Indian Valley, Seeläsgen, Willow Creek, Avoca and Obernkirchen. Full, or almost full, recrystallization is seen in, e.g., Bingera, Dungannon, Kokstad, Durango, Willamette, Joel's Iron and Social Circle. The deformation and the subsequent annealing probably took place when the meteorites were still buried as part of the parent bodies.

Some meteorites with recrystallized kamacite show a new generation of Neumann bands throughout all the recrystallized grains. Cedartown is a fine example. The Neumann bands probably date from the final breakup of the parent body. Other, smaller irons display virtually

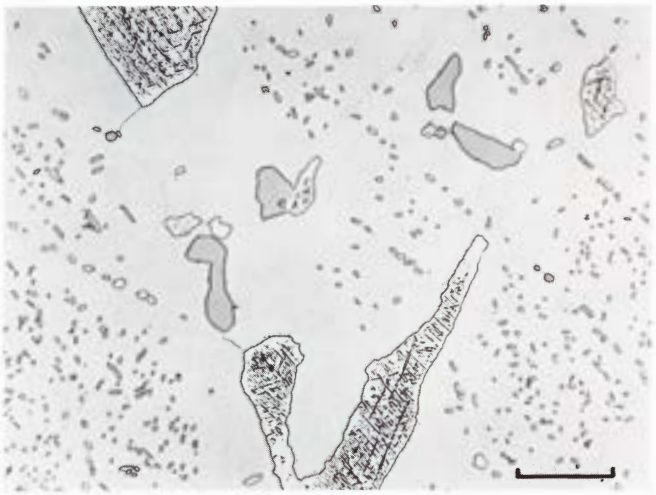

Figure 222. Dalton (U.S.N.M. no. 1010). A medium octahedrite which was thoroughly annealed in space. The kamacite shows cellular structure and includes numerous spheroidized taenite particles. Schreibersite is gray. For an enlarged view of the taenite see Figure 223. Etched. Oil immersion. Scale bar 20 μ.

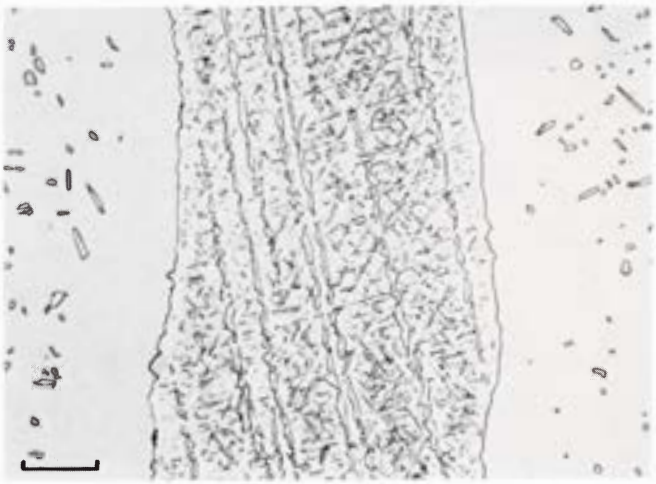

Figure 223. Dalton (U.S.N.M. no. 1010). A taenite lamella under decomposition to a fine-grained $\alpha + \gamma$ composite due to cosmic annealing. The larger α-particles are arranged along (111) planes of the taenite. A few 2 μ schreibersite particles are also seen. Etched. Oil immersion. Scale bar 10 μ.

undamaged recrystallized kamacite grains. This is the case, e.g., with Social Circle, Zerhamra, Cachiyual and Ruff's Mountain. It may cautiously be concluded that in certain instances, the parent body can have disintegrated without Neumann band formation in the kamacite phase. The reason may be that earlier large scale cracks had significantly decreased the coherence of the parent body.

The kamacite of many meteorites displays an extremely fine-grained duplex mixture of α and γ. See, e.g., Jamestown, Maria Elena, Sandtown, Chilkoot and Davis Mountains. It appears that the duplex structures were formed by the annealing of shocked ϵ-structures which were supersaturated with respect to nickel. The annealing must have required relatively low heating and cooling rates and probably occurred inside the parent body.

2. Taenite. Reheating of taenite will, when slow, tend to eliminate its steep nickel gradients by diffusion. Cosmically reheated iron meteorites are thus of inferior value for studies of the primary cooling rate.

Meteorites which exhibit recrystallized or duplex kamacite will usually contain visibly altered taenite. This altered taenite may be termed spheroidized although the spheroidization is rarely perfect. It appears that plastically deformed taenite can decompose to $\alpha + \gamma$ along the slipplanes. The precipitating α is submicroscopic at first, but by prolonged annealing it becomes coarser and finally coalesces to blebs, neatly arranged along the slipplanes. Thorough annealing will entirely spheroidize the taenite-kamacite texture. Good examples of imperfect spheroidization are to be found in, e.g., Willamette, Dalton, Durango, Zerhamra and Joel's Iron. In Maria Elena, Reed City and Seneca Falls the spheroidization is better, and in Hammond it has almost completely eliminated the original Widmanstätten structure. The annealed taenite is usually softer than 200 HV.

Brief reheating of taenite to above 700 or 800° C softens and alters the appearance under the microscope in a different way. Carbon, previously in solid solution in the taenite, redistributes itself, and subsequent rapid cooling produces bainitic-martensitic structures in the adjacent metal. This aspect is further discussed under, e.g., Kayakent and Cape York.

The cloudy or stained taenite simultaneously becomes clear and yellow, often via an intermediate mosaic structure. See Figure 114. Apparently the reason is the alteration of preexisting submicroscopic $\alpha + \gamma$ mixtures to homogeneous γ that remains metastable on subsequent rapid cooling. Examples are legion in the heat-affected rim zones but may also be found in shock-reheated Canyon Diablo samples.

The microhardness of taenite with 30-35% Ni in Cape York is displayed in Figure 113. Taenite requires a significantly longer time than kamacite to regain its initial,

Figure 224. View Hill (U.S.N.M. no. 3196). A portion of a large troilite inclusion. Recrystallization to 5 μ grains has occurred near the edge, while the interior shows undulatory extinction. Polished. Crossed polars. Scale bar 100 μ.

annealed state. It is, however, interesting to note that the hardness of thoroughly annealed taenite (30-35% Ni) is the same as that of annealed kamacite (7% Ni), 155±5.

3. Troilite. As noted above, troilite may selectively melt at hot spots in the shocked meteorite; if it is diluted by adjacent kamacite or minerals, it solidifies in eutectic structures. If barely melted and unpolluted from the surroundings, it may solidify to an assemblage of equiaxial grains which are randomly oriented. The more foreign material included in the melt, the finer the equiaxial texture. It cannot be ruled out that some of the equiaxial structures were produced by solid state transformation at high temperature or by recrystallization. A thorough study of the troilite is required and the Hugoniot curve should be constructed. Troilite with equiaxial "recrystallized" structure is designated "4" in Appendix 1. It was probably formed by pressure-temperature conditions intermediate between the twinned troilite "2" and the shock-melted eutectics "5."

4. Schreibersite and Rhabdite. Relatively slow reheating will tend to reduce the nickel content of the phosphides according to the equilibrium diagram and will also partly spheroidize and dissolve the phosphides. Small taenite particles will usually become segregated along the kamacite-phosphide interface as is clearly seen, e.g., in Ballinoo and Willow Creek. The effects are probably associated with reheating inside the parent body but, sometimes, perhaps with orbital reheating.

Severe, but brief, reheating produces unequilibrated phosphide-kamacite interfaces, with "thorns" projecting out from the phosphide into the surrounding metal. These thorns are apparently phosphorus-rich subboundaries. The structures are found in the heat-affected α_2 zone from the atmospheric flight and in a few shock-reheated fragments, notably Canyon Diablo samples of stage V.

Still more intense shock-reheating results in partial recrystallizaton and finally in selective melting (Canyon Diablo stage VI-VII). Melting also occurs in the exterior 50% of the heat-affected α_2 flight zone (Figure 45).

5. Carbides. Cohenite and haxonite probably formed as metastable minerals in the later parts of the primary cooling period (page 124). If subsequent deformation resulted in internal and interphase cracks, it appears likely that slight reheating to perhaps 400 or 500° C could decompose the carbides to graphite and kamacite. During the present study, all stages of carbide decomposition have been detected in different irons. For example, in group I, Cosby's Creek, Youndegin and Bischtübe contain perfect cohenite, while on the other hand Bohumilitz, Shrewsbury and Wichita County display partially decomposed cohenite. Dungannon and Oscuro Mountains no longer contain cohenite, but the texture of the graphite-kamacite assembly clearly shows that cohenite was the precursor mineral. The precipitated kamacite has grown in a peculiar way, as

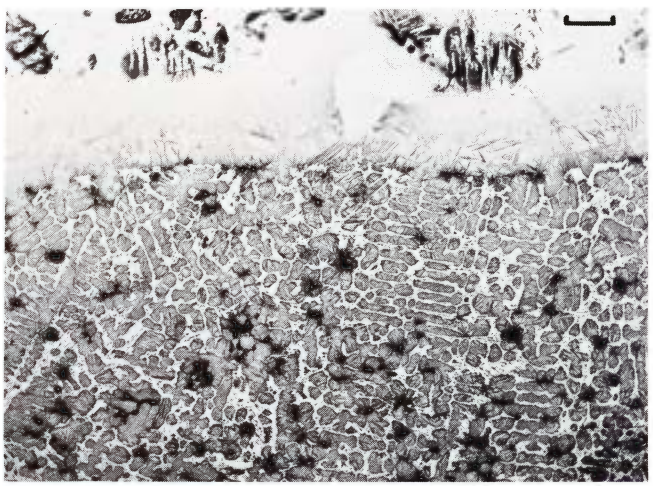

Figure 226. Canyon Diablo. Shock-reheated fragment in which the cohenite-schreibersite aggregates have been completely melted. They solidified rapidly to steaditic structures. See also Figure 227. Etched. Scale bar 100 μ.

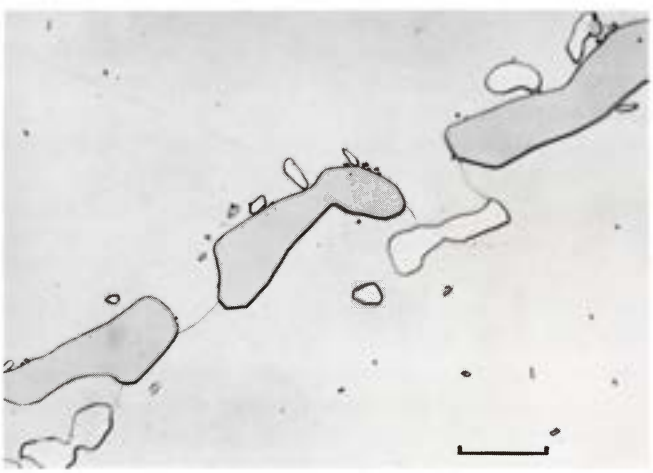

Figure 225. Willamette (U.S.N.M. no. 333). The three grain boundary particles of schreibersite are slightly spheroidized due to annealing in space. Small taenite particles (white) were simultaneously separated. Etched. Oil immersion. Scale bar 20 μ.

Figure 227. Deatil of Figure 226. The austenitic dendrites were sufficiently rich in carbon and nickel to transform to acicular martensite upon cooling. The phosphorus-rich eutectic appears black after etching with neutral sodium picrate. Scale bar 20 μ.

elongated columnar grains with a preferential orientation. See Figures 737 and 1930.

In group III, carbides are rare, but they are present in the small subgroup discussed on page 102. Rhine Villa, Coopertown, Staunton and Tanakami Mountains have undecomposed haxonite, while Kokstad, Matatiele and Willow Creek display graphite lamellae and kamacite inside the plessite in a texture that clearly indicates that haxonite was the precursor mineral.

The decomposition structures were probably caused by slow annealing on the parent body. The decomposition observed in the newest member of the group, Paneth's Iron, was, however, caused by artificial reheating.

Brief reheating, like that which occurs in the atmospheric rim zone or in small shock-reheated Canyon Diablo fragments (stage V-VI), causes momentary recrystallization, particularly along shear zones, and decomposition of cohenite starts at the kamacite-cohenite interphase. A wave of carbon atoms are sent into the surrounding metal which, because of the reheating, is in the austenitic state. Upon subsequent cooling the carbon-rich austenite transforms to bainitic-martensitic structures as discussed on page 54 and elsewhere. The carbon-rich transformation zones stand out as prominent black halos around the cohenite; see Figures 270 and 1181.

Upon severe, but brief reheating, above about 1100° C, the cohenite melts selectively, then dissolves part of the surroundings. Subsequent rapid cooling produces ledeburitic structures. Examples are known from Canyon Diablo (stage VII) and from the heat-affected rim zone of, e.g., Arispe and North Chile.

Concluding Remarks

Although the material is as yet rudimentary, it should – with the general information developed above – be possible in principle to distinguish between the various modes of deformation and reheating. However, the story is very complex because a shocked or annealed structure is rarely the result of one cycle only, but usually the end result of the combined effect of several deformation and reheating events. The time interval between these events is at present difficult to estimate. However, by selecting a series of genetically related meteorites with a wide range of structures it might be possible by a combination of structural and gas-analytical techniques to arrive at a better understanding. The following examples from group IIIA would be suited for such analyses: Cape York, Kenton County, Morito, Davis Mountains, Chilkoot, Uwharrie, Plymouth, Willamette, Roebourne, Seneca Falls and Juromenha. Or examples from group IIA are: Coahuila, Calico Rock, Murphy, North Chile, Boguslavka, Braunau, Cedartown, Uwet, Holland's Store, Mejillones and Bingera.

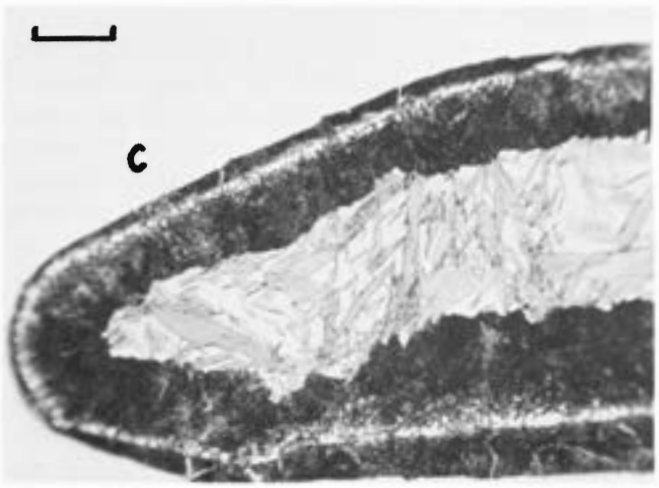

Figure 228. Odessa, artificially reheated to 850° C for 10 minutes, then air-cooled. The cohenite (C) originally enveloped kamacite. Carbon from the decomposed cohenite caused bainite (black) and acicular martensite to form in the kamacite. The white line indicates the original kamacite-cohenite interface. Etched. Scale bar 100 μ.